Posted on 9 Mar 2023 — The copyright holder is the author/funder. All rights reserved. No reuse without permission. — https://doi.org/10.22541/essoar.167839712.21210255/v1 — This a preprint and has not been peer reviewed. Data may be preliminary.

Hillslope-channel Coupling in a Changing Permafrost Landscape: the Critical Role of Water Tracks

Joanmarie Del Vecchio[1]

[1]Affiliation not available

March 9, 2023

Joanmarie Del Vecchio[1,2], Simon Zwieback[3], Joel C. Rowland[4], Roman A. DiBiase[5,6], Marisa C. Palucis[1]

[1]Department of Earth Science, Dartmouth College, Hanover, NH, USA

[2]Neukom Institute for Computational Science, Dartmouth College, Hanover, NH USA

[3]Department of Geosciences, University of Alaska Fairbanks, Fairbanks, AK USA

[4]Earth and Environmental Sciences Division, Los Alamos National Laboratory, NM USA

[5]Department of Geosciences, Pennsylvania State University, University Park, Pennsylvania 16803, USA

[6]Earth and Environmental Systems Institute, Pennsylvania State University, University Park, Pennsylvania 16803, USA

Corresponding author: Joanmarie Del Vecchio (joanmarie@dartmouth.edu)

Key Points:

- Seasonal and long-term permafrost thaw change hillslope hydrology and erodibility
- Satellites observe surface displacements concentrated in certain landscape positions
- A conceptual model is proposed for hillslope-channel coupling in permafrost landscapes mediated by water tracks

Abstract

The Arctic is experiencing rapid climate change, and the effect on hydrologic processes and resulting geomorphic changes to hillslopes and channels is unclear because we lack quantitative models and theory for landscape evolution in thawing permafrost. The presence of permafrost modulates water infiltration and flow and the stability of soil-mantled slopes, implying there should be a topographic "signature" of permafrost processes, including warming-driven disturbance. To inform predictions of hillslope-channel dynamics under changing climates, we examined soil-mantled hillslopes within a ~ 300 km^2 area of the Seward Peninsula, western Alaska, where discontinuous permafrost is particularly susceptible to thaw and rapid landscape change. In this study we pair high-resolution topographic and satellite data to multiannual observations of InSAR-derived surface displacement over a five-year period to quantify spatial variations in topographic change across an upland landscape. We find that neither basin slope nor the presence of knickzones controls the magnitude of recent surface displacements within the study basin, as may be expected under conceptual models of temperate hillslope evolution. Rather, the highest displacement magnitudes tended to occur at the broad hillslope-channel transition zone. In this study area this zone is occupied by water tracks which are zero-order ecogeomorphic features that concentrate surface and subsurface flow paths. Our results suggest

Posted on 9 Mar 2023 — The copyright holder is the author/funder. All rights reserved. No reuse without permission. — https://doi.org/10.22541/essoar.167839712.21210255/v1 — This a preprint and has not been peer reviewed. Data may be preliminary.

that water tracks, which we hypothesize occupy hillslope positions between saturation and incision thresholds, are vulnerable to warming-induced subsidence and incision. We expect gullying within water tracks to outpace infilling by hillslope processes, resulting in growth of the channel network under future warming.

Plain Language Summary

Climate and ecology can shape hillslopes and the extent of river networks by controlling how much water is available for erosion. These forces also control whether water can erode soil if it is strengthened by ice or roots. The permeability and stability of permafrost hillslopes changes with seasonal and long-term warming due to frozen ground's impermeability and resistance to erosion. This link between temperature and erosion in permafrost landscapes is thus more direct than most geomorphic models developed at lower latitudes presume. We related the locations of satellite topographic change to the geomorphic processes that dominate that part of the landscape based on the shape of the hillslopes and valleys. This allows us to determine whether the pattern of disturbance across the landscape is related to geomorphic variables like slope or climate-modulated variables like soil saturation. We find that displacement of the ground surface preferentially occurs within water tracks, features that straddle the hillslope-channel transition and concentrate surface and subsurface flow paths. Changes in climate and vegetation in permafrost landscapes are potentially driving water tracks to transition into true channels, expanding the channel network.

Introduction

Understanding the physical relationships that set hillslope-channel transitions and drainage density can reveal erosion mechanisms operating on the landscape (Perron et al., 2008; Sweeney et al., 2015), which in turn impact water chemistry (Littlefair et al., 2017; Shakil et al., 2022) and soil carbon storage (Yoo et al., 2005; Shelef et al., 2017; Turetsky et al., 2020). Because geomorphic models predict that the areal extent of the valley network is sensitive to climate variables like precipitation and vegetation (Istanbulluoglu and Bras, 2005; Sangireddy et al., 2016), determining the factors that set hillslope-valley transition can help predict landscape response to perturbations. One of the most dramatic Earth system perturbations is the amplified warming of high latitudes and potential degradation of permafrost landscapes and ecosystems in the Anthropocene (Natali et al., 2021). Permafrost, or perennially frozen ground, cycles through annual phases of thaw in the upper 10s of centimeters, termed the active layer. In this layer water and nutrients flow freely during the summer before freezing again in the fall. Disruptions to water, solute and sediment fluxes at high latitudes have particularly dire consequences for the global carbon budget and feedbacks on climate warming (Turetsky et al., 2020). Soil-mantled hillslopes occupy approximately one fifth of Northern Hemisphere land affected by permafrost (Shelef et al., 2017), yet we know little about the dynamics of hillslope-channel coupling in permafrost landscapes (Tananaev, 2022) compared to temperate landscapes and therefore cannot predict how climate change will alter surface processes and carbon release (Shelef et al., 2017; Wohl, 2018).

Permafrost landscapes have distinctive boundary conditions compared to their temperate counterparts that could affect hillslope-channel coupling. Phase changes from frozen to unfrozen water alter the permeability and erodibility of permafrost soils (French, 2018), which in turn modulates water infiltration and flow and the stability of soil-mantled slopes (Walvoord and Kurylyk, 2016; Lewkowicz and Way, 2019). Factors like soil cohesion and depth to an impermeable layer in soil therefore vary not only in space but also in time, on both seasonal and millennial timescales (Rowland et al., 2010). In upland permafrost landscapes, discharge has historically been seasonal, peaked, and ephemeral as winter snow storage and spring melt dictate much of the discharge (Bring et al., 2016). Vegetation and the impermeable permafrost mediate the flow of water on the surface and shallow subsurface (Walvoord and Kurylyk, 2016).

The interaction of slope processes, hillslope hydrology and vegetation communities of permafrost landscapes implies that there could be a topographic "signature" of permafrost processes in the areal extent of channel networks, which are thought to be closely tuned to the mechanical and hydrologic properties of the underlying

Posted on 9 Mar 2023 — The copyright holder is the author/funder. All rights reserved. No reuse without permission. — https://doi.org/10.22541/essoar.167839712.21210255/v1 — This a preprint and has not been peer reviewed. Data may be preliminary.

geology, soils, and climate (Abrahams and Ponczynski, 1984; Sangireddy et al., 2016; Litwin et al., 2022). Moreover, since rates of landscape evolution should also be sensitive to climate-driven changes in hydrology and temperature (Matsuoka, 2001), it is possible that a signature of warming-driven disturbance exists in the form of changing drainage networks as hillslope and channel dynamics respond to changing climate (Rowland et al., 2010). However, the remoteness of high-latitude landscapes has been a barrier to establishing heuristic models of their evolution, and there are few landscape evolution models that describe permafrost landscape dynamics, and none incorporate tundra vegetation. Additionally, whereas catastrophic events like thaw slumps and thermokarst landslides are well-documented in the Arctic (e.g. Balser et al., 2014; Lewkowicz and Way, 2019; Witharana et al., 2022), subtle topographic change associated with steadier surface processes remains understudied.

Here we focus on soil-mantled hillslopes on the Seward Peninsula of western Alaska, which are underlain by discontinuous permafrost and sensitive to warming-induced thaw (Jafarov et al., 2018). We explore drivers of slope instabilities documented in the field in previous observations (Del Vecchio et al., 2023) and newly documented displacement patterns via Interferometric Synthetic Aperture Radar (InSAR). InSAR displacements appear insensitive to spatially variable basin slopes driven by knickzone migration. Instead, displacement trends reflect dynamics in the transitional zone between hillslopes and channels, which in this landscape is occupied by water tracks - linear, zero-order geomorphic features that concentrate surface and subsurface flow paths in permafrost uplands (Kane et al., 1989; Trochim et al., 2016; Evans et al., 2020). We show how our new framework of water tracks as geomorphologic agents can explain the mismatch between field observations of low drainage densities in landscapes underlain by permafrost (Mcnamara et al., 1999; Luoto, 2007) versus model results predicting the opposite (Bogaart et al., 2003). We also speculate how observed topographic change in the water track regime may portend changes to fluvial networks in thawing permafrost landscapes.

Background: Hillslope-channel interactions in permafrost landscapes

The relative extent of the diffusive erosion regime on hillslopes can distinguished from the advective erosion regime of river channels by examining the areal extent of the channel network and by the location of scaling breaks in slope-area pots (Figure 1). Two frameworks exist to describe this process transition. In the first, the rate of runoff-driven incision at channel heads outpaces valley infilling by diffusive processes (Montgomery and Dietrich, 1989; Perron et al., 2008). Channel heads are also thought to form where geomorphic thresholds are surpassed (Tucker and Bras, 1998; Wohl, 2018), including the erodibility of substrate or vegetation (Istanbulluoglu and Bras, 2005) (Figure 1). In both process-competition and threshold frameworks, climate parameters should affect the balance of hillslope and fluvial processes by controlling the amount of water available for geomorphic work as well as the biotic and abiotic factors for creating and moving soil (Hales and Roering, 2007; Sangireddy et al., 2016).

Posted on 9 Mar 2023 — The copyright holder is the author/funder. All rights reserved. No reuse without permission. — https://doi.org/10.22541/essoar.167839712.21210255/v1 — This a preprint and has not been peer reviewed. Data may be preliminary.

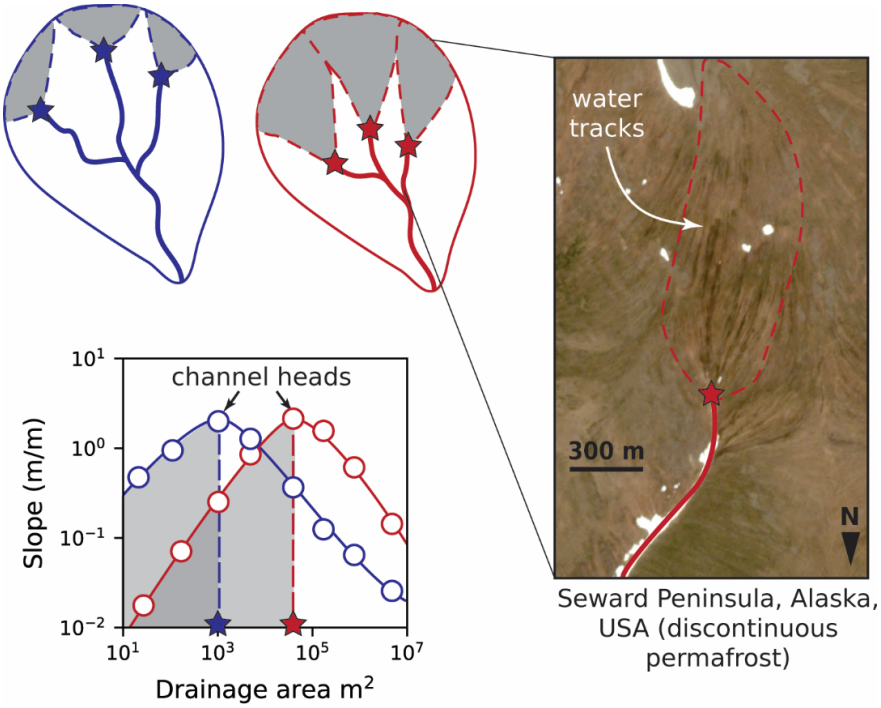

Figure : Conceptual diagram for the relationship between slope-area relationships and drainage density in landscapes with different balances of advective and diffusive processes. Two cartoon watersheds exhibit high (blue) and low (red) drainage densities based on the location of the channel heads (stars). Scaling breaks in plots of local slope versus upslope contributing area (shown as white points binned by drainage area with parabolic fits) indicate the drainage area at which the diffusive and advective processes are equally effective at transporting sediment and the transition between convex and concave hillslope areas. In western Alaska on the Seward Peninsula, the convex hillslopes upslope of channel heads are often drained by water tracks, shown in visible imagery in June 2019 PlanetScope imagery.

In temperate climates soil diffusivity has limited dependence on mean annual temperature (MAT) (Hurst et al., 2013; Perron, 2017); however, field and experimental data indicate higher soil transport rates in permafrost landscapes that are further amplified by warming (Harris et al., 1997; Matsuoka, 2001; Del Vecchio et al., 2023). During cold periods, significant shear may occur at the base of the active layer where liquid water persists in the pore space at ground temperatures slightly below 0°C (Lewkowicz and Clarke, 1998; Shur et al., 2005), with instantaneous shear rates up to one order of magnitude higher than shear measured in temperate soils (Carson and Kirkby, 1972). As mean annual temperature increases, permafrost thaw events are associated with increased hillslope sediment flux driven by thermokarst (Lewkowicz and Harris, 2005; Lewkowicz, 2007; Gooseff et al., 2009). In the Arctic, this signature of increased hillslope sediment flux is also observable in the increased sedimentation of floodplains and offshore basins occurred during past warming events (Mann et al., 2010; Kaufman et al., 2016; Tesi et al., 2016). Modern observations of Arctic hillslopes show that both unusually warm and wet conditions promote slope failures, and that the frequency of failures is increasing with recent warming (Balser et al., 2014; Lewkowicz and Way, 2019). Changing high-latitude hydroclimate may also change the timing and extent of tundra soil saturation, in which earlier infiltration will saturate low-conductivity soil layers what were once frozen in early spring (Walvoord and Kurylyk, 2016), or shifting discharge timing from spring snowmelt to summer rainfall (Bintanja and Andry, 2017).

Water fluxes from hillslopes to streams are often controlled by water tracks, zero-order geomorphic features that concentrate surface and subsurface flow paths connecting upland and lowland water fluxes (Tananaev, 2022). Water in water tracks flows within the active layer above the permafrost table, concentrating water

Posted on 9 Mar 2023 — The copyright holder is the author/funder. All rights reserved. No reuse without permission. — https://doi.org/10.22541/essoar.167839712.21210255/v1 — This a preprint and has not been peer reviewed. Data may be preliminary.

in both wetter landscapes of Alaska (Trochim et al., 2016), the polar deserts in the Canadian High Arctic (Paquette et al., 2017), and the dry valleys of Antarctica (Levy et al., 2011; Levy and Johnson, 2021). Because the organic mat within a water track is saturated all summer, the thermal conductivity of the water track is higher compared to the surrounding hillslopes, leading to enhanced thaw in and around the track (Kane et al., 2001; Trochim et al., 2016; Evans et al., 2020). Water tracks can occur in the absence of topographic valleys (Hastings et al., 1989; McNamara et al., 1999) and are perhaps analogous to rills in sparsely vegetated arid landscapes. Water tracks tend to self-organize into parallel, rather than dendritic, networks, where the flow path and rate depends both on surface topography and on the thickness of the porous organic horizon (Hinzman et al., 1991; Trochim et al., 2016).

Trochim et al (2016) showed that water tracks could be classified into five distinct ecomorphological categories, primarily controlled by surficial geology and vegetation community. Geologic and ecologic factors that affect channel development in temperate landscapes may also modulate permafrost landscape channelization but with the additional complexity of feedbacks with the frozen ground below these flowpaths. Water track stratigraphy revealed that water tracks have evolved different vegetation communities over time, which Trochim et al. (2016) attributed to adjustments to prevailing climate conditions. Water track morphology and vegetation assemblage thus adapt over time to changing hydrologic and thermal regimes (Jorgenson et al., 2010), such that a permanent flowpath is maintained.

McNamara et al (1999) investigated self-organization and self-similarity of drainage networks (Rodríguez-Iturbe et al., 1992; Tarboton et al., 1992) in the foothills of the Brooks Range, Alaska and found that, paradoxically, Arctic drainage networks are either quite dense if water tracks are considered as part of the drainage network, or quite sparse if they are not. The authors found that water tracks initiate at or around the drainage area at which slope-area relationships would indicate a change from divergent to convergent topography (slope is maximized compared to drainage area). However, a significant portion of the landscape (drainage areas between 3 x 10^3 and 1 x10^4 m^2) support gentler slopes than convex hillslope as drainage area increases but do not support incised fluvial channels. They conclude that water tracks are energetically efficient flowpaths that occupy a flow regime that is transitional between the purely hillslope drainage and the fluvial channels that characterize the bottom of the valley. Other field studies found the high infiltration capacity of peat soils controlled high-latitude drainage density more so than temperature or geology (Luoto, 2007). In Nome Creek near Fairbanks, dispersed channel-forming flows on deep active layers, plus widespread moss cover, is thought to inhibit hillslope incision (Crawford et al., 2014).

In an alternative conceptualization of drainage development in frozen ground, the presence of permafrost limits the subsurface storage of water on hillslopes, and thus the channel network expands upslope at the onset of cold climate periods and contracts during warming, and hillslope material diffuses into the now-unoccupied hollows (Bogaart et al., 2003; Wohl, 2018). Although the Bogaart et. al (2003) model sets a constant hillslope diffusivity with changing climate to argue for network contraction during warming, most other permafrost landscape evolution models drive hillslope transport by the thermal state of the soil column. In these models, frozen material is assumed immobile, and soil movement under saturated permafrost conditions occurs at a higher rate than diffusive processes in unsaturated soil, resulting in maximum flux when MAT ˜0degC (Kirkby, 1995; Andersen et al., 2015; Bovy et al., 2016a).

Site description and prior work

To investigate coupled hillslope-channel response to permafrost thaw, we document topographic and vegetation characteristics on soil-mantled hillslopes on the Seward Peninsula, western Alaska, broadly located around the former Sullivan Camp (65deg3'47"N 166deg11'43"W) (Figure 2). The study area, in the western Seward Peninsula in western Alaska, is underlain by the Precambrian Nome Group, comprised of chlorite and marble schists, and the Precambrian Slate of the York region, which contains metamorphosed interbedded dolomitic and argillaceous slates. Both units are in places intruded by coarse-grained gabbros and diabases (Sainsbury, 1972), expressed as rocky unvegetated areas or bedrock tors on the surface. Unglaciated hill-

Posted on 9 Mar 2023 — The copyright holder is the author/funder. All rights reserved. No reuse without permission. — https://doi.org/10.22541/essoar.167839712.21210255/v1 — This a preprint and has not been peer reviewed. Data may be preliminary.

slopes support a rocky, thin (up to 1-2 m) soil mantle that is often organized into solifluction lobes and sweeping terraces (Kaufman et al., 1989). LGM glaciation is limited to the Kigluaik Mountains to the south of the study area, but earlier Pleistocene glaciation may have been more extensive and reached some portions of the study area (Kaufman et al., 2011).

There is little variation in bedrock geology or climate between studied subbasins, but there is spatial variability in basin steepness that may be caused by base level change. The study region is bordered by the Imuruk Basin to the east and Port Clarence to the north, both of which drain into the Bering Sea to the west, which underwent large changes in sea level during the last glacial period (Elias et al., 1996; Lozhkin et al., 2011). The region has also seen extensive dredging for gold, which may also affect stream incision and subsequent hillslope response. In the center of the study area, at the confluence of the Bluestone River and Gold Run, the stream is cutting into the surrounding hillslopes creating a scarp of ˜150 m. This location, as well as a section downstream on Gold Run and upstream on the Bluestone River, are associated with over-steepened channel reaches, or knickzones (Figure 2a). These knickzones contribute to a steepening of adjusting subbasins (Bigi et al., 2006), resulting in spatial variability of basin-averaged slopes (Figure S1).

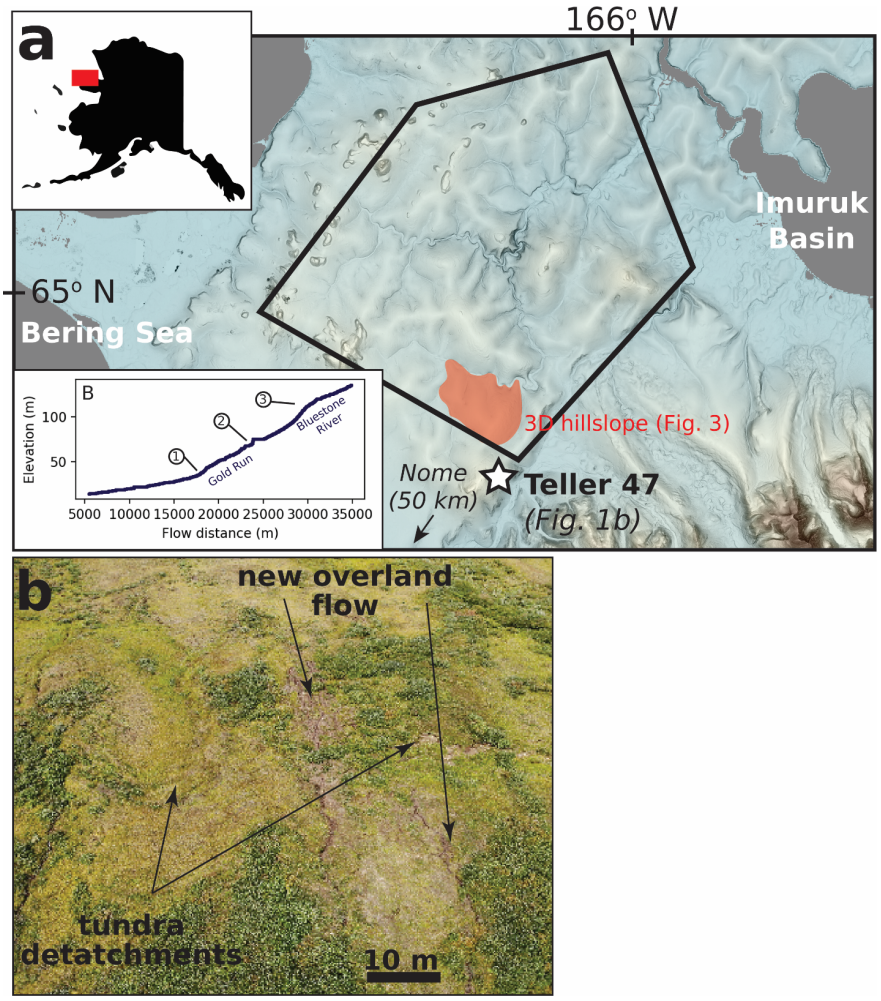

Figure Site locations on the Seward Peninsula, western Alaska. (a) A regional slopeshade map showing the location of the Teller 47 watershed site (Del Vecchio et al., 2023) as well as the nearby hillslopes used in the current analyses. The glaciated Kigluaik Mountains are to the southeast of the study area. A

Posted on 9 Mar 2023 — The copyright holder is the author/funder. All rights reserved. No reuse without permission. — https://doi.org/10.22541/essoar.167839712.21210255/v1 — This a preprint and has not been peer reviewed. Data may be preliminary.

longitudinal river profile of the main drainages, the Bluestone River and Gold Run, demonstrate convexities (or knickzones) at elevations between 50-100 m asl. (b) Aerial imagery from August 2019 at the Teller 47 site demonstrating ongoing slope disturbances, including lobate and arcuate failure surfaces and new overland flow on the tundra. Average slope of the topography here is ˜0.32 m m^{-1} (˜18°).

The study area is underlain by discontinuous permafrost, and the mean annual air temperature for the region from 1980-2015 has been - 6°C with a positive trend of 0.06 °C per year (Thornton et al., 2017; Jafarov et al., 2018). Over the same period, total average rain and snow precipitation is ˜400 and 300 mm per year, respectively; snow precipitation has declined while rain precipitation has increased.

Prior work at an instrumented watershed adjacent to our study area, a relatively steep (15-20°) ˜ 1.7 km^2watershed about 60 km NW of Nome ("Teller 47"), provides field context and validation for the remote observations presented herein (Del Vecchio et al., 2023) (Figure 2a). Multiannual surface displacements from repeat GPS surveys find average inter-annual movement of 5-10 cm, though many targets moved >10 cm between 2018 and 2019. Interannual surface soil velocities measured through differential GPS imply high hillslope diffusivities in permafrost landscapes compared to temperate landscape measurements, in line with modeled assumptions of high shear rates in thawing permafrost (Kirkby, 1995; Bovy et al., 2016). Total movement is weakly positively correlated to slope, except on steep, rocky slopes with thin soil mantles where displacements were low, implying soil thickness and/or drainage also plays a role in surface velocity. InSAR-derived ground displacement on nearby hillslopes show that cumulative summer displacement mirrored cumulative summer rainfall for the years 2017-2019 (Alaska State Climate Center), whereas intra- and interannual temperature trends did not relate to displacement. An intense rainfall event in August 2019 resulted in soil piping, mud ejection features and overland flow at the surface, which disturbed the surface of the tundra and underlying soil (Figure 2b), including the transport of 10 cm cobbles. Gully head retreat and bank collapse are ongoing, though the areas around the drainages appear to be permafrost-free. Disturbances to the tundra surface mapped from drone imagery clustered in slope-area space (Del Vecchio et al., 2023, Figure 6).

On hillslopes in the broader study area, drainage areas between 10^3 and 104 m^2 are broadly consistent with the pattern of water tracks, taking the characteristic curvilinear pattern of water tracks observed in imagery (Evans et al., 2020) and occupying a sizeable portion of the convex-up hillslopes between ridgelines and topographic valleys (Figure 3). As in other locations in the wetter western Arctic, water tracks in the area support tussock tundra communities dominated by cottongrass ("tussocks"), peat moss and dwarf birch and willows (Walker et al., 1989).

Posted on 9 Mar 2023 — The copyright holder is the author/funder. All rights reserved. No reuse without permission. — https://doi.org/10.22541/essoar.167839712.21210255/v1 — This a preprint and has not been peer reviewed. Data may be preliminary.

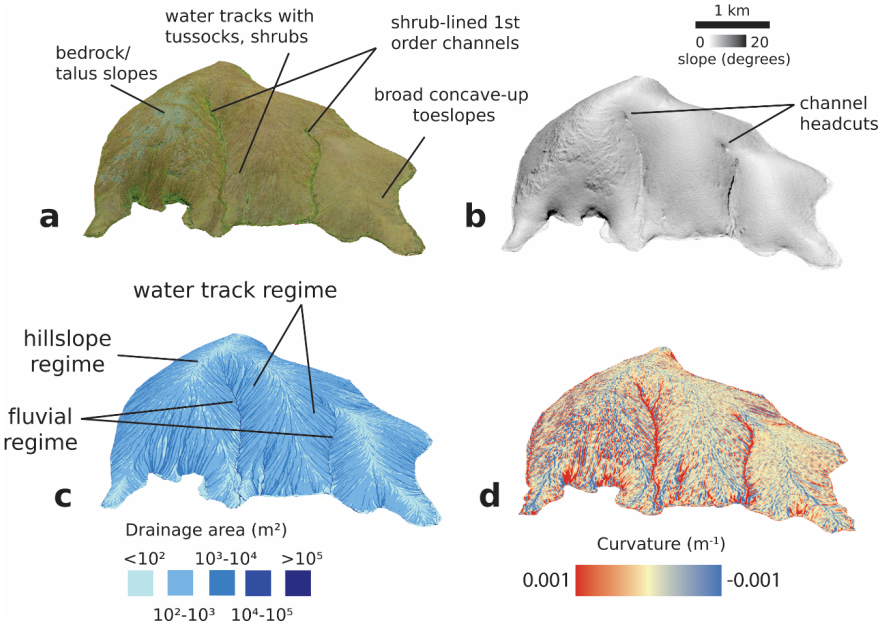

Figure A perspective view of a typical soil-mantled hillslope in the study area (see Figure 2). (a) A satellite view reveals spatial variation in vegetation type (vibrant green colors at high drainage areas are tall shrubs whereas dull greens are tussocks and mosses with some dwarf shrubs) and rocky slopes. The brown curvilinear streaks across the hillslope are water tracks. (b) A slopeshade view reveals a contrast in surface roughness between the rocky and soil-mantled slopes, which lack incision aside from two first-order channels. Sharp notches in the hillslope are channel headcuts, marking the initiation of fluvial processes. (c) A map of drainage area delineate water track paths in drainage areas of 10^3-10^4 m^2. The three process regimes discussed in this text – hillslope, water track, and fluvial – are also indicated. (d) Long-wavelength curvature, in which positive values are concavities (valleys).

Methods

We combined InSAR-derived displacement observations with topographic analysis on soil-mantled hillslopes on the Seward Peninsula to upscale observations from the Teller 47 site to the landscape scale. We used morphometric indicators of landscape form and disequilibrium to determine whether displacements were concentrated at particular drainage areas, as was observed in field data at the Teller 47 site (Del Vecchio et al., 2023). We explore whether and how patterns of displacement relate to regional steepness gradients driven by baselevel change. We hypothesize that if all regional hillslopes experience channel extension and slope failures like the Teller 47 site, this would imply a climate-controlled change. If there were spatial patterns to hillslope-channel form, disturbance dynamics may instead be driven by lithologic contrasts and/or base level changes. If there was no pattern and a small portion of hillslopes were experiencing topographic change (e.g. <5% as may be expected from frequent storm events as estimated by Parker et al., 2016), these dynamics may be driven by stochastic erosion events that go through cycles of filling and evacuation similar to temperate-climate hollows (Reneau and Dietrich, 1991; Hales et al., 2012; Parker et al., 2016). By sampling a variety of hillslope and channel forms, we eliminate subbasin-specific peculiarities to generate an average view of the landscape (Grieve et al., 2016).

Posted on 9 Mar 2023 — The copyright holder is the author/funder. All rights reserved. No reuse without permission. — https://doi.org/10.22541/essoar.167839712.21210255/v1 — This a preprint and has not been peer reviewed. Data may be preliminary.

InSAR

We estimated multiannual surface movements across the study area landscape by analyzing InSAR (Interferometric Synthetic Aperture Radar) observations from the ALOS-2 satellite. InSAR is sensitive to motion along the line of sight (LOS), which will contain contributions from downslope and surface-perpendicular movements at any given location. We consistently adopt the sign convention that positive movements correspond to increasing LOS distance between the satellite and the surface (i.e., subsidence is positive displacement).

Surficial geology map

A ˜20 x 8 km subset of the InSAR multiannual displacement dataset was selected that covered soil-mantled slopes. To contextualize the study area and analyze the regional remote sensing results, we created a regional geomorphic map. We used the bedrock and Quaternary map of Kaufman (1989) to map the Kigulaik Mountain bedrock and associated glaciofluvial deposits in the southeast corner of the InSAR coverage. Beyond the 1989 map, we used a slope map generated from the 2 m ArcticDEM digital elevation model (DEM) (Porter et al., 2018) of the region to demarcate between fluvial/alluvial channels and plains, soil-mantled hillslopes, bedrock outcrops, coastline and water bodies (Figure S2). We used bedrock outcrops as reference points for zero displacement when constructing the regional interferogram (see 4.1.2).

Multiannual movement

Multiannual displacements from 2015-2019 were estimated from ALOS-2 satellite data (Suzuki et al., 2012) at a resolution of 40 m. The images were acquired in mid-July (2015-07-16, 2016-07-14, 2017-07-13, 2019-07-11), allowing us to estimate multiannual displacements with limited aliasing from seasonal movements. The line-of-sight direction was from the west (-104 degrees azimuth angle) at a mean incidence angle of 31 degrees. On east-facing/west-facing slopes, downslope movements and surface-perpendicular subsidence contributed with the same/opposite sign to the observed LOS displacement.

We estimated the inter-annual displacement velocity using an InSAR time series approach. We first formed and unwrapped (Chen and Zebker, 2001) short-baseline (Berardino et al., 2002) interferograms with temporal separations of up to three years from the four mid-July images (2015-2017, 2019). We referenced the interferometric phases at bedrock outcrops, which were assumed to be stable. We then estimated the movement time series from the interferogram stack by weighted least squares, with the weights determined by an estimate of the speckle-induced variance (Zwieback and Meyer, 2021). The final mean inter-annual displacement velocity and its standard error were determined by fitting a linear deformation model to the movement time series.

We performed quality controls on the data by manually masking areas where the results were deemed unreliable due to unwrapping errors. We noted that errors and subsequent masked areas increased significantly with the inclusion of the 2019 image, and thus we concentrate our analyses in the main on averaged displacements deriving from the 2015-2017 imagery only and document data incorporating the 2019 data in the Supplement. Being both coarse resolution and an interannual average, our InSAR-derived displacements underestimated the extensive erosion we observed in August 2019 compared to 2018, and the storm's effects are eliminated entirely when we use 2015-2017 imagery only.

Topographic analyses

Topographic analysis was performed using the 2-m-resolution ArcticDEM, a digital surface model of the Arctic derived from optical stereo imagery (Porter et al., 2018). We used the mosaiced ArcticDEM product, in which individual stereopair DEMs have been co-registered, blended, and feathered to reduce edge-matching artifacts. Topographic slope and aspect were calculated on a DEM resampled to 10 m to eliminate the effects of microtopography.

Posted on 9 Mar 2023 — The copyright holder is the author/funder. All rights reserved. No reuse without permission. — https://doi.org/10.22541/essoar.167839712.21210255/v1 — This a preprint and has not been peer reviewed. Data may be preliminary.

We calculated simple topographic metrics from the 2 m topography using LSDTopoTools (Clubb et al., 2014; Mudd et al., 2021) with a circular window of radius 14 m (a scale we selected to smooth microtopography and noise in ArcticDEM) to calculate slope and curvature. To better characterize distributed flow networks on planar to convex hillslopes, we used the d-infinity flow-routing algorithm to calculate drainage area (Tarboton, 1997). To compensate for data rasters of variable resolution (e.g., InSAR displacement of resolution 40 m, slope of resolution 10 m), we extracted the coordinate of the center of each 2 m pixel on the DEM and sampled each topographic metric at that coordinate.

We used channel and basin delineation tools in LSDTopoTools to extract the channel network and define low-order drainage basins in the study area. Because the watershed algorithm uses a D8 (steepest-descent) flow routing and results in artifacts on convex hillslopes, we eliminated small watersheds (< 100 m^2) from our analyses. Using the extracted coordinate data, we then determined which coordinates fell in each basin and calculated basin-averaged metrics like slope and displacement magnitude.

We collected slope-area information about channel heads in the study area by manually mapping the location of 120 channel heads resolved by the 2 m-resolution ArcticDEM. To locate channel heads, we used as basemaps the long-wavelength curvature and hillshade rasters calculated by LSDTopoTools to locate the discrete headcut associated with the heads of the channel network. We performed the manual mapping because the algorithmic approaches within LSDTopoTools produced unsatisfactory results (too many false positives and offset from headcuts visible in hillshades). We also collected four manually delineated topographic transects (i.e., elevation as a function of distance) from hillslope ridgelines through the headwaters of a first-order channel to examine hillslope morphometry and its relationship to InSAR-dervied displacements.

To determine the geomorphic regime in which the highest displacement occurs for a given watershed, we created binned slope-area plots for each of the 190 basins we analyzed. Based on observations of the drainage areas associated with water tracks and channel heads, and following the observations of McNamara et al (1999), we manually assigned each basin a label for the geomorphic regime at which high displacements were concentrated: "hillslope" (concentrated in drainage areas of $< 10^2$ m^2 and/or increasing slope with increasing drainage area), "water tracks" (10^2-10^4 m^2), "fluvial" (based on channel head contributing areas of $>10^4$ m^2), or "indeterminate" if there was no pattern or if there was more than one locus of high displacements. Water tracks were present in all basins analyzed.

Because InSAR displacements are measured along the line-of-sight direction, the aspect of the analyzed basins strongly influenced the magnitude of displacement (Figure S3). To account for this bias, we binned each basins' pixels into eight cardinal and ordinal directional bins, rotated slightly to align with the LOS (e.g. "west" is between 234.5° and 279.5° to align with the LOS of the satellite at 257°). We then calculated displacement z-scores for each pixel within these eight directional bins (in which the difference between the mean displacement of each directional bin and an individual pixel's displacement is divided by the standard deviation of the aspect's displacements) and calculated the mean z-score for pixels within each basin, allowing us to observe basins experiencing particularly high or low displacement regardless of aspect. We also calculated the elevation of the basin outlet. We compared both basin-averaged slope and basin outlet elevation to basin-averaged displacement to test whether basin steepening due to knickpoint migration influences short-term displacement on the hillslopes.

The collection period of the imagery used in the Seward Peninsula ArcticDEM spans from 2011 to 2017, whereas the primary InSAR data were averaged from 2015-2017. There is potentially a temporal mismatch between the location of headcuts visible on ArcticDEM and offsets observed in InSAR. If headcuts observed on ArcticDEM migrated upslope as we observed in the field in 2019, the two datasets may be overestimating the distance between maximum displacements observed via InSAR and channel headcuts. Both photogrammetry-derived topography and InSAR may be biased in and around channels by the presence of thick riparian vegetation.

Posted on 9 Mar 2023 — The copyright holder is the author/funder. All rights reserved. No reuse without permission. — https://doi.org/10.22541/essoar.167839712.21210255/v1 — This a preprint and has not been peer reviewed. Data may be preliminary.

Results

Hillslope-scale results

Hillslopes in the study area are broad and exhibit few areas of valley-scale concavities. As measured in the four hillslope profiles (Figure 4), the distance between hilltop and initiation of the channel network (located via positive curvature occurring along lines of steepest descent) ranges from 1500 to 2000 m. In cross-section, hillslopes are convex-up and channels are either concave-up (e.g., profiles 2 and 3) or straight (profiles 0 and 1).

For the four hillslope profiles, the zone of maximum InSAR-derived displacements occurs roughly halfway between the channel head and ridgeline. The profiles were selected such that the azimuth between the surface normal and the LOS direction remained roughly constant, thus minimizing spurious trends in the InSAR displacements.

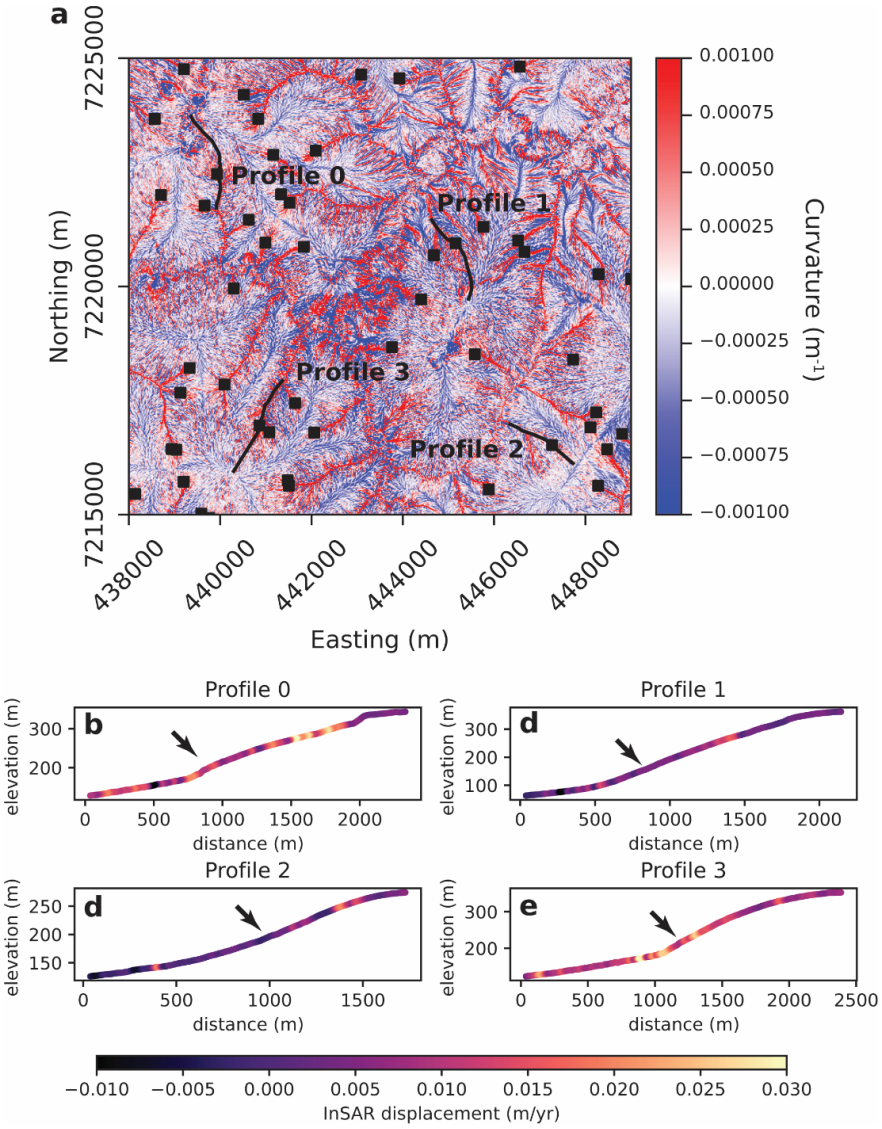

Figure Hillslope-scale results of InSAR displacements. (a) location of four transects shown in B-E overlain on a map of curvature. Black lines are transects. Black squares are manually mapped channel heads. (b-e) Topographic transects from ridgeline to first-order channel demonstrating transition between convex and concave topography, colored by InSAR displacement. Location of channel head shown as black arrow pointing to hillslope profile.

Basin controls on short-term displacement

There does not appear to be a spatial pattern in displacement z-scores across the study area (Figure 5a). Neither basin-average slope nor outlet elevation correlates with InSAR-derived displacement magnitudes (Figure 5b). Basin slope varies across the study area, likely related to the presence of over-steepened river reaches (Figure S1); despite the tendency for rivers to steepen in response to channel steepening at their toes (Bigi et al., 2006), this adjustment does not seem to impact displacement on the hillslopes since displacements do not appear sensitive to either slope or to basin outlet elevation (a proxy for base-level adjustment). Although much of the InSAR data around the steep banks of Gold Run was masked due to low data quality, the pixelwise displacements that are unmasked are not particularly high compared to surrounding hillslopes (Figure S4). Displacement is also insensitive to basin size.

Posted on 9 Mar 2023 — The copyright holder is the author/funder. All rights reserved. No reuse without permission. — https://doi.org/10.22541/essoar.167839712.21210255/v1 — This a preprint and has not been peer reviewed. Data may be preliminary.

Posted on 9 Mar 2023 — The copyright holder is the author/funder. All rights reserved. No reuse without permission. — https://doi.org/10.22541/essoar.167839712.21210255/v1 — This a preprint and has not been peer reviewed. Data may be preliminary.

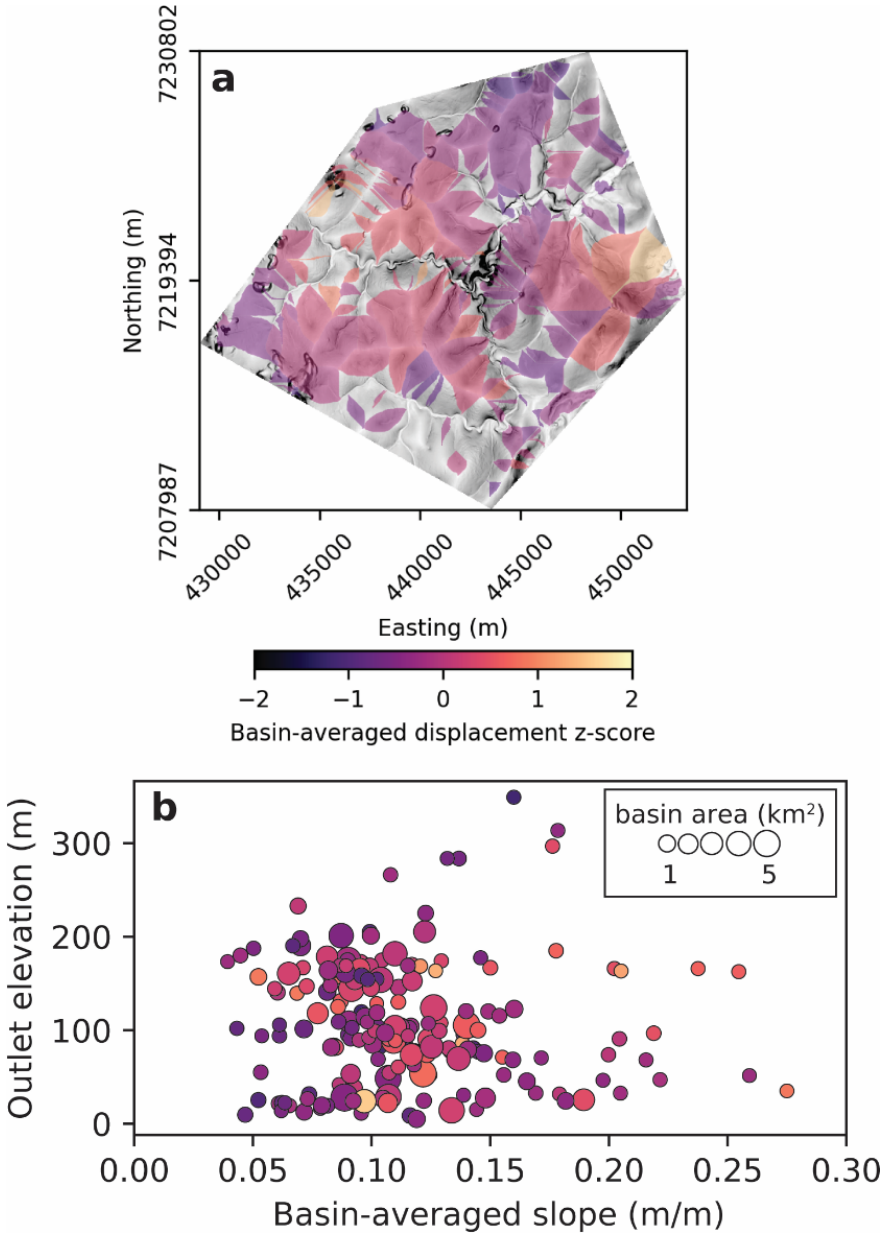

Figure Basin-averaged displacement versus morphometric properties. (a) Basins are grouped by aspect and assigned z-scores to overcome look-direction bias in basin-averaged displacement as measured by InSAR. There is no clear spatial trend to basins with high or low z scores in the study area. (b) While basin-averaged slope appears influenced by watershed outlet (a proxy for whether it may be adjusting to the migrating knickpoint), degree of adjustment to the knickzone (reflected in basin-averaged slope) has no bearing on displacement z score.

Morphology versus displacement

The inflection point in slope-area plots for all points in the landscape occur at drainage areas of about 1 x10^3m^2, which corresponds to the transition from convex-up hillslopes to concave-up valleys (Figure 6). In

Posted on 9 Mar 2023 — The copyright holder is the author/funder. All rights reserved. No reuse without permission. — https://doi.org/10.22541/essoar.167839712.21210255/v1 — This a preprint and has not been peer reviewed. Data may be preliminary.

agreement with observations from McNamara et al (1999), water tracks occupy drainage areas associated with the inflection point in the slope-area plot, but fluvial channels with defined banks occur at higher drainage areas (>10^4 m^2; Figure 6a). Curvature increases with drainage area, indicating increasing concavity with increasing contributing area (Figure 6b). Above contributing areas of ˜10^4 m^2, however, curvature increases rapidly, indicating further widening and deepening that may be associated with gullies and valleys.

The inflection point in slope-area space also corresponds to the highest displacements for each drainage area bin (Figure 6a). Displacements are highest in the drainage area bins leading up to this inflection point, and displacements begin to decrease at drainage areas greater than the inflection point. The convex-up hillslope portion of the landscape exhibits higher displacements than the fluvial portion of the landscape.

The binned drainage areas of highest displacement derived from InSAR overlap with the drainage areas of the UAV-mapped tundra disturbances at the Teller 47 site (Del Vecchio et al., 2023), although most of the study area's hillslope angles are not as steep as the mapped failures.

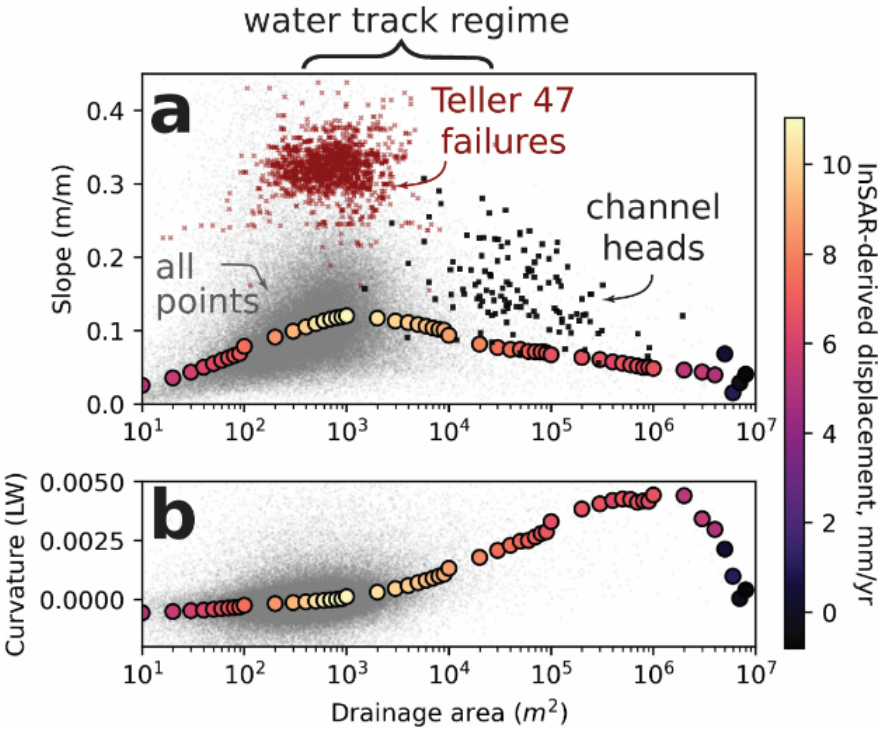

Figure Morphometric control on zones of highest surface displacement. (a) Landscape pixels (gray) binned by mean slope and colored by InSAR displacement. Drainage areas consistent with water tracks in planform view of the landscape (Figure 3) are highlighted. Slope-area information shown from Teller 47 hillslope failures (Del Vecchio et al., 2023) and manually mapped channel heads. (b) Mean curvatures with each drainage area bin demonstrate transition between convex (negative curvatures) and concave (positive curvatures) landscape positions versus displacement.

The highest mean displacements correspond to intermediate slopes (0.18-0.20 m m^{-1}, or ˜11°) at drainage areas ˜10^3 m^2(Figure 7a). Interestingly, pixels with the steepest slopes in the landscape (>0.3 or >17°) are associated with lower displacement magnitudes than lower-sloping pixels of similar drainage areas. This is in contrast to the sub-meter scale displacements mapped at the Teller 47 site, where disturbances were concentrated between slopes of 0.25-0.4 m m^{-1} (14° to 22°), though without field validation it is difficult to know if the two disturbance mechanisms are related. Additionally, displacements on steeper slopes are more sensitive to changes in drainage area. However, there is considerable noise in these data.

Posted on 9 Mar 2023 — The copyright holder is the author/funder. All rights reserved. No reuse without permission. — https://doi.org/10.22541/essoar.167839712.21210255/v1 — This a preprint and has not been peer reviewed. Data may be preliminary.

We also break out displacement data by aspect, focusing on north- and south-facing pixels (Figure 7b). These two directions are orthogonal to the look direction of the satellite and thus do not have any inherent biases, allowing us to examine how aspect might modulate displacement. On average, south-facing pixels have higher displacements than north-facing pixels, especially in drainage areas between 10^2-10^4 m^2, but once again there is considerable overlap in the two datasets.

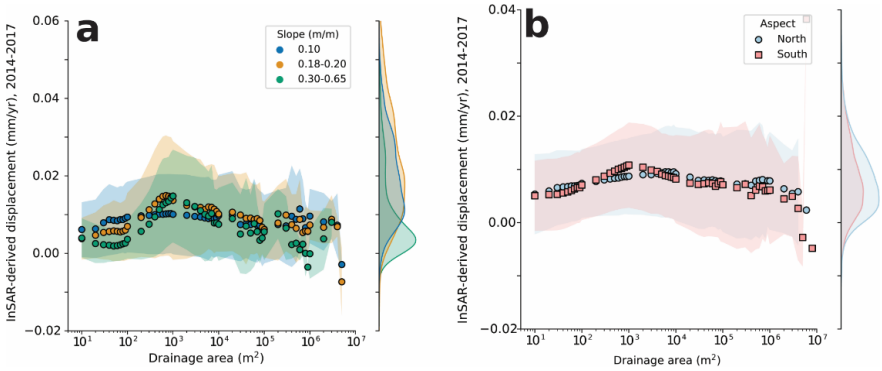

Figure : Displacement patterns as a function of drainage area modulated by (a) slope and (b) aspect. Envelopes around data are 1 standard deviation. Histograms to the right of the scatterplots show frequency of displacement measurements across all drainage area bins.

In map view, areas of high InSAR-derived displacements often co-occur with hillslope positions containing water tracks (Figure 8a). Of the 190 basins, 125 had a single clear locus of high displacements in certain drainage areas, and 69 of those basins (36%) experienced heightened displacements in the water track regime, 18 had high displacements concentrated in hillslope areas, and 38 had high displacements concentrated in fluvial areas (Figure S5). Taking watersheds >0.5 km^2 (n=55), eliminating particularly narrow basins comprised of just a few water tracks, 44% of basins were characterized by water track-dominated displacement. When including all basins, basins with water track-dominated displacements had higher median z-score displacements than watersheds with other loci of displacement (Figure 8b). We found significantly higher displacement z-scores than watersheds with displacement concentrated in the fluvial regime ($p<0.001$ in a Mann-Whitney U-test; Charlier et al., 2022). There was no spatial pattern to basins with displacement locations, and there was no relationship between basin outlet elevation or basin-averaged slope and zone of highest displacement (Figure S5).

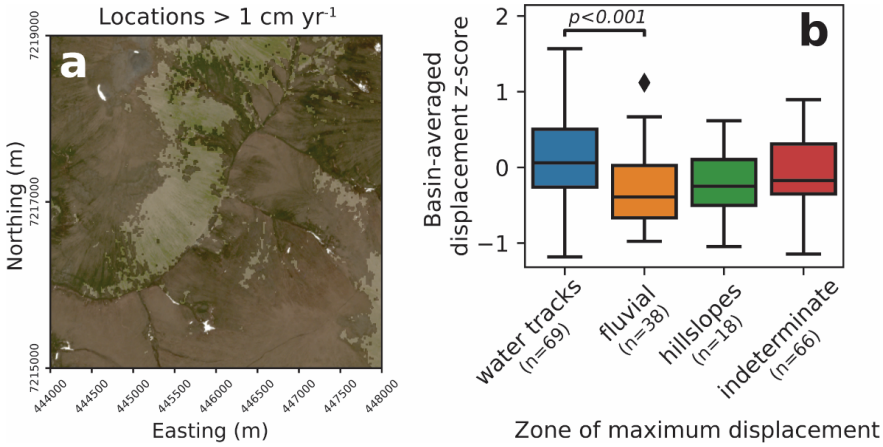

Figure : Water tracks are associated with higher InSAR-derived displacement. (a) Map of landscape positions

Posted on 9 Mar 2023 — The copyright holder is the author/funder. All rights reserved. No reuse without permission. — https://doi.org/10.22541/essoar.167839712.21210255/v1 — This a preprint and has not been peer reviewed. Data may be preliminary.

in which displacements averaged > 1 cm/yr superimposed on June 2019 true-color imagery from Planet's Dove satellites. (b) Boxplots demonstrating range of all basin-averaged displacement z-scores binned by the geomorphic regime in which maximum displacement in the basin occurs. Mann-Whitney U-tests showed significantly higher displacements magnitudes in basins dominated by displacement in the water track regime over fluvial regime displacement.

Discussion

Relationship with prior field observations

Like McNamara et al (1999), we observed in our regional analysis that water tracks and outlets for overland flow can transmit water without incising through tundra to mineral soil. The similarities between observations made in this study and the Brooks Range foothills of McNamara et al (1999) are significant in that the latter is underlain by continuous permafrost and had a thinner active layer at the time of their field observations, as well as having hillslopes comprised of glacial till. These concordances indicate that the relationship between hillslope interflow, water tracks and fluvial incision may be broadly applicable to tussock tundra permafrost environments regardless of permafrost continuity and summer active layer depth.

Our observations of topographic displacements aligns with drainage areas associated with slope failures and other advective processes observed on the soil-mantled hillslopes at the Teller 47 site (Del Vecchio et al., 2023). A majority of aerially mapped failures at the Teller 47 site occurred between 0.5-10 x 10^3 m^2, with proportionally more of the hillslope with contributing areas 5-10 x 10^3 m^2 containing failures. These failures included arcuate slope failures, fluvial incision into the tundra, and head retreat of existing gullies. In contributing areas from 1-10 x 10^3 m^2, pipeflow had undermined the tundra mat, flowing within, and mobilizing, mineral soil, resulting in emergence of flowpaths at the surface and coating tundra sedge in sediment. However, the failures at Teller 47 occurred on hillslope positions with steeper slopes (14° to 22°) than the majority of slope angles our study region; in our study site steep slopes were not necessarily associated with the highest displacement magnitudes (Figure 7a). Although topographic displacements observed in InSAR might not be permanent and/or discrete erosion events, field observations and InSAR-derived surface movement maps both reflect displacements preferentially occurring within the broad hillslope-channel transition regime where advective processes may temporarily overtake diffusive ones. Displacement could also be the result of subsidence as ground ice melts and deflates the soil column, and subsequent freezes do not restore the increase volume associated with frozen versus liquid water in soil profiles. Either displacement action would work to lower the elevation of these locations on the hillslope overtime, leading water to flow even more to these locations, setting off gully formation and headward incision (Evans et al., 2020).

Role of permafrost landscape processes on steady state hillslope-channel form

High hillslope fluxes and low channel density driven by permafrost processes

The broad hillslopes and low drainage densities in the study area are consistent with previous observations in permafrost landscapes (Mcnamara et al., 1999; Luoto, 2007; Crawford et al., 2014) and imply a dominance of diffusive sediment transport processes over advective (fluvial) ones (Perron et al., 2009). The high surface velocities measured at the Teller 47 site imply high volumetric sediment fluxes (Del Vecchio et al., 2023), which would inhibit channel formation. If channel-forming discharge events are infrequent enough, as might be expected if snowmelt-derived discharge peaks when soils are still frozen in the early summer (Walvoord and Kurylyk, 2016), soil diffusion would eliminate the incipient channels and smooth over topographic lows (Montgomery and Dietrich, 1989).

In hillslopes positions with drainage areas between 10^3-10^4 m^2, including broad concave-up toeslopes, slope decreases with drainage area, which is typical of channels, but most parts of the landscape with these drainage areas are occupied by planar hillslopes and water tracks. Unlike heuristic models of hillslopes that

Posted on 9 Mar 2023 — The copyright holder is the author/funder. All rights reserved. No reuse without permission. — https://doi.org/10.22541/essoar.167839712.21210255/v1 — This a preprint and has not been peer reviewed. Data may be preliminary.

steepening with distance from the divide to accommodate increasing volumes of upslope material (Gilbert, 1909), these hillslope positions may instead be moving via earthflow-like transport and/or are not being excavated efficiently by fluvial processes, leading to accumulation.

Water tracks as zero-order basins

Water tracks act as conveyors of saturated subsurface, and sometimes surface, flow without resulting in the long-wavelength concavities across the hillslope reminiscent of colluvial hollows or valleys (Grieve et al., 2018). When they emerge downslope of ridgelines, water tracks in our study area quickly self-organize into parallel, linear preferential flow paths and continue downslope for hundreds of meters before coalescing into a valley or joining a higher-order stream at the hilltoe. In a geomorphic framework, these water tracks may occupy the topographic space in between a saturation and incision threshold (Tucker and Bras, 1999). Water tracks emerge where there is sufficient upslope contributing area (draining either snowmelt, rainfall, or thawed ground ice) to coalesce into channelized, saturated flowpaths. This concentration of water promotes subsidence of, but not necessarily incision into, the underlying tundra mat and mineral soil. Only when tracks have large enough watersheds or coalesce to produce a sufficiently large upslope drainage area (in this study, between 10^4 - 10^6 m^2; Figure 6a) do these flowpaths have sufficient erosive energy to incise deep (> 1 m) gullies and channels and generate the channel heads we mapped.

Based on our observations we propose that on these soil-mantled permafrost hillslopes, the combined effect of an erosion threshold from tundra vegetation and high hillslope diffusivities overpowers the effects of reduced storage of subsurface water in the presence of a permafrost table to lengthen hillslopes and reduce drainage density. At steady state permafrost conditions (consistent active layer thickness and snowfall-dominated runoff), water tracks transmit water between a runoff threshold and erosion threshold drainage area, and any topographic lows that form from stochastic slope failures or incipient gullying are quickly smoothed out by high soil transport rates.

Hillslope-scale morphology on Seward Peninsula likely represents the integration of many thousands of years of climate conditions. Soil thickness and sediment discharge from hillslopes may respond quickly to climate base level perturbations, but hillslope form takes much longer to adjust. Hillslope relaxation times operate on timescales longer than the typical glacial-interglacial cycle, especially for hillslope lengths relevant to our study area ([?]100 m) (Fernandes and Dietrich, 1997; Perron, 2017). This was exemplified in the (Bovy et al., 2016b) study, which posited that soil thickness could respond to climate changes on the order of ˜10^5 yrs, but not hillslope form. Since most of our study area has remained unglaciated through the Quaternary with minor portions glaciated in the Mid-Pleistocene (Kaufman et al., 2011), the vast hillslopes are almost certainly a product of millennia of permafrost processes.

Active geomorphology on the Seward Peninsula: Base level or climate?

Lack of base level control on short-term displacements

It is important to distinguish between climatic and non-climatic drivers of hillslope instability and new channel incision. Changing bedrock river erosion rates can also lead slopes to fail via undercutting and drive channel heads upslope as fluvial processes outcompete hillslope processes (DiBiase et al., 2015; Bigi et al., 2006). If spatial patterns of displacement were attributed to a wave of bedrock river incision traveling through the network, we would expect to see both over-steepened river reaches and high displacements at roughly the same elevation (Lague, 2014). However, we showed in our analyses that channel form and outlet elevation (proxies for relative influence of knickzone migration) as well as basin-averaged slope (a morphologic consequence of such a knickzone) are unrelated to any patterns in where displacements occur within a basin nor the absolute magnitude of those displacements. Displacements associated with the central gorge are also not higher than surrounding hillslopes upstream of base level change (Figure S4).

Posted on 9 Mar 2023 — The copyright holder is the author/funder. All rights reserved. No reuse without permission. — https://doi.org/10.22541/essoar.167839712.21210255/v1 — This a preprint and has not been peer reviewed. Data may be preliminary.

Stochastic zero-order basin dynamics versus climate response

Are disturbances within the water track regime in one-third to one-half of the studied basins indicative of a climate response, or just the result of stochastic erosion events? Due to their location between hillslope and channel positions, water tracks could be analogous to colluvial hollows that fill and evacuate when they have reached some critical soil thickness in which a rainfall event would cause slope failure (Reneau and Dietrich, 1991; Parker et al., 2016). In this framework a portion of hollows would fail depending on their morphologic properties (mostly slope) and thickness of colluvial fill, which would be controlled by sediment diffusivity and time since last failure. Parker et al (2016) found that up to 10% of saturated colluvial hollows in southern Appalachia would fail in storms with a 20-year return period and up to 60% would fail in storms with a 200-year return period.

Because saturated hydraulic conductivities and root cohesion, critical elements to the analyses performed by Parker et al. (2016), are under-constrained in our field site, it is impossible to perform the analyses that would provide insight into the frequency with which we may observe failures in the water track regime. However, the rainstorm of August 2019, the largest rainstorm to have occurred in the study interval, has approximately a 50-year return period (Alaska Climate Research Center). The soil creep transport coefficients in our study site may be 1-6x higher than that of the southern Appalachians as reported by Parker et al.. (Del Vecchio et al., 2023), and by their nature water track topography is at or close to saturation (Trochim et al., 2016). Achieving critical soil depths for instability must not be a limiting factor in stability of water tracks on the landscape; otherwise the water track regime could not persist long-term. Instead, the most important modulator of slope stability would be the cohesion term in water tracks, which is likely high due to both seasonal freeze and root cohesion. Warming would reduce the cohesion imparted by ground ice, and climate change may indirectly drive vegetation change (Myers-Smith et al., 2011) that could lower root cohesion.

Conversely, if water tracks always maintain higher resisting forces than driving forces with respect to slope stability, the only other driver of disturbance in the water track regime would arise from the overcoming of an incision threshold due to either (1) an increase in water depth or (2) a decrease in cohesion imparted by vegetation or ground ice (Istanbulluoglu and Bras, 2005). Water depth increase is related to climate in the size of individual rain or melt events, as is loss of cohesion from thawing ground ice.

Based on this study, we propose that the water track regime has evolved to remain largely stable under long-term vegetation, ground thaw and discharge conditions, and any disturbance (incision or slope failure) in the water track regime is quickly annealed by high hillslope transport rates. However, changes to water track cohesion in the form of ground ice thaw and/or vegetation change could promote the types of displacements we observe in our study, especially if surface flows are more frequent and voluminous due to increased water from precipitation and/or ground ice thaw.

Implications for thawing permafrost landscapes

In the recent past, hillslopes on the Seward Peninsula often experienced peak runoff conditions while the active layer was thin as snowmelt arrived in late spring. On the Snake River outside Nome, Alaska, peak daily discharge since the 1960s has occurred either in June or August, driven by snowmelt or rainfall, respectively (US Geological Survey, 2016). In the future, however, less precipitation may fall as snow and more precipitation may fall as rain across the Arctic (Bintanja and Andry, 2017; Landrum and Holland, 2020), which would make late-season peak discharge, as occurred in 2019, the new normal for soil-mantled hillslopes in western Alaska. If the current extent of the fluvial network represents the long-term balance between hillslope diffusion and fluvial incision, then sustained higher summer precipitation could drive more overland flow and extend the channel network uphill. In particular, areas of hillslopes occupied by water tracks are likely to be geomorphically dynamic in the future. Independent of any new incision or slope failures, deeper thaw combined with more rain and less snow may cause sustained subsidence of the ground under water tracks (Evans et al., 2020). Inter-track water tables, no longer perched by shallow permafrost tables, would respond by falling, potentially sapping shallower water tracks of interflow and lead flowpaths

Posted on 9 Mar 2023 — The copyright holder is the author/funder. All rights reserved. No reuse without permission. — https://doi.org/10.22541/essoar.167839712.21210255/v1 — This a preprint and has not been peer reviewed. Data may be preliminary.

to coalesce (Lamontagne-Halle et al., 2018). Coalescing water tracks would lead to more voluminous, deeper flows and thus further promote incision into hillslopes.

Under a warming climate, earlier seasonal thaw may also lead to increased soil moisture in low-conductivity soil layers that were previously frozen during high infiltration during snowmelt (Walvoord and Kurylyk, 2016), increasing the chances of undermining the mineral soil under the tundra mat. Early thaw coincident with peak flow not only allows water to incise into mineral soil, but it allows for maximum leaching of mineral-associated carbon within organic horizons (Hirst et al., 2022). The net C loss from this process is amplified if deeper thaw liberates old carbon for dissolution and transport (Schwab et al., 2020) since photomineralization of dissolved organic carbon (DOC) derived from permafrost produces CO_2 at twice the rate of modern DOC undergoing the same process (Bowen et al., 2020). We therefore expect water tracks to continue as a source of greenhouse gas beyond their already-outsized role in permafrost landscapes (Harms et al., 2020).

Conclusions

In this study we reconciled divergent field and modeling observations of permafrost landscape form by studying soil-mantled hillslopes on the Seward Peninsula, western Alaska, where thaw of discontinuous permafrost generates dynamic landscape change. Our landscape-wide morphometric analysis of soil-mantled permafrost hillslopes reveals that the hillslope-channel transition is a spatially diffuse and hydrologically distinct zone. Water tracks occupy the geomorphic regime where water transits the landscape through the tundra mat without generating valleys, thereby lengthening hillslopes and reducing drainage density. The water track regime also corresponds to the area of highest InSAR-derived surface displacements in many watersheds, and across the entire study area.

We compared satellite-derived measures of surface displacement to topographic metrics to show that certain slope-area regimes underwent more topographic change than others, and we compared our findings in this study to previous field observations of discrete slope failures (Del Vecchio et al., 2023). We find that the water track regime underwent more topographic change from 2014-2017 than the hillslope or fluvial regimes in the same landscape, but these landscape positions are likely not experiencing the discrete slope failures we observed in steeper landscape positions. However, our results are consistent with subsidence (Evans et al., 2020) and disturbance within water tracks due to lower incision thresholds from deepening active layers and the shift in timing of peak discharge. Because water tracks are vulnerable to warming-induced erosion and incision, we expect water fluvial networks on permafrost hillslopes to expand under future climate and vegetation change.

Acknowledgements

J. D. was supported by the Office of Science Graduate Student Research (SCGSR) Program from the Department of Energy and the Neukom Institute for Computational Science at Dartmouth College. J.D. is grateful for discussions with Sarah Evans, Shawn Chartrand, and Joe Levy, which improved this manuscript.

Open Research

Topographic data for study area is available from the ArcticDEM project (version 3 mosaics; https://doi.org/10.7910/DVN/OHHUKH). Derived topographic datasets were generated by the LSDTopoTools2 software package (https://doi.org/10.5281/zenodo.5788576). The configuration file for this analysis is provided, along with other scripts and large raster files for analysis, on GitHub (https://doi.org/10.5281/zenodo.7708691). Scripts for InSAR analyses are located at https://doi.org/10.5281/zenodo.7542485.

Posted on 9 Mar 2023 — The copyright holder is the author/funder. All rights reserved. No reuse without permission. — https://doi.org/10.22541/essoar.167839712.21210255/v1 — This a preprint and has not been peer reviewed. Data may be preliminary.

References

Abrahams, A.D., and Ponczynski, J.J., 1984, Drainage density in relation to precipitation intensity in the U.S.A.: Journal of Hydrology, v. 75, p. 383–388, doi:10.1016/0022-1694(84)90061-1.

Alaska State Climate Center Alaska Climate Research Center Data Portal:, https://akclimate.org/data/ (accessed February 2022).

Balser, A.W., Jones, J.B., and Gens, R., 2014, Timing of retrogressive thaw slump initiation in the Noatak Basin, northwest Alaska, USA: Journal of Geophysical Research: Earth Surface, v. 119, p. 1106–1120, doi:10.1002/2013JF002889.

Bigi, A., Hasbargen, L.E., Montanari, A., and Paola, C., 2006, Knickpoints and hillslope failures: Interactions in a steady-state experimental landscape, *in* Tectonics, Climate, and Landscape Evolution, Geological Society of America, doi:10.1130/2006.2398(18).

Bintanja, R., and Andry, O., 2017, Towards a rain-dominated Arctic: Nature Climate Change, v. 7, p. 263–267, doi:10.1038/nclimate3240.

Bogaart, P.W., Tucker, G.E., Vries, J.J.D., and de Vries, J.J., 2003, Channel network morphology and sediment dynamics under alternating periglacial and temperate regimes: A numerical simulation study: Geomorphology, v. 54, p. 257–277, doi:10.1016/S0169-555X(02)00360-4.

Bovy, B., Braun, J., and Demoulin, A., 2016, A new numerical framework for simulating the control of weather and climate on the evolution of soil-mantled hillslopes: Geomorphology, v. 263, p. 99–112, doi:10.1016/j.geomorph.2016.03.016.

Bowen, J.C., Ward, C.P., Kling, G.W., and Cory, R.M., 2020, Arctic Amplification of Global Warming Strengthened by Sunlight Oxidation of Permafrost Carbon to CO2: Geophysical Research Letters, v. 47, p. e2020GL087085, doi:10.1029/2020GL087085.

Charlier, F. et al., 2022, trevismd/statannotations: v0.5:, doi:10.5281/zenodo.7213391.

Clubb, F.J., Mudd, S.M., Milodowski, D.T., Hurst, M.D., and Slater, L.J., 2014, Objective extraction of channel heads from high-resolution topographic data: Water Resources Research, p. 5375–5377, doi:10.1002/2013WR014979.Reply.

Crawford, J.T., Stanley, E.H., and Stanley, E.H., 2014, Distinct Fluvial Patterns of a Headwater Stream Network Underlain by Discontinuous Permafrost: Arctic, Antarctic, and Alpine Research, v. 46, p. 344–354, doi:10.1657/1938-4246-46.2.344.

Del Vecchio, J., Lathrop, E., Dann, J.B., Andresen, C.G., Collins, A.D., Fratkin, M.M., Zwieback, S., Glade, R.C., and Rowland, J.C., 2023, Patterns and rates of soil movement and shallow failures across several small watersheds on the Seward Peninsula, Alaska: Earth Surface Dynamics Discussions, p. 1–28, doi:10.5194/esurf-2022-43.

Evans, S.G., Godsey, S.E., Rushlow, C.R., and Voss, C., 2020, Water Tracks Enhance Water Flow Above Permafrost in Upland Arctic Alaska Hillslopes: Journal of Geophysical Research: Earth Surface, v. 125, p. 1–18, doi:10.1029/2019JF005256.

French, H.M., 2018, The Periglacial Environment: Hoboken, NJ, John Wiley & Sons Ltd, 515 p.

Gooseff, M.N., Balser, A., Bowden, W.B., and Jones, J.B., 2009, Effects of hillslope thermokarst in Northern Alaska: Eos, v. 90, p. 29–30, doi:10.1029/2009EO040001.

Grieve, S.W.D., Hales, T.C., Parker, R.N., Mudd, S.M., and Clubb, F.J., 2018, Controls on Zero-Order Basin Morphology: Journal of Geophysical Research: Earth Surface, v. 123, p. 3269–3291, doi:10.1029/2017JF004453.

Posted on 9 Mar 2023 — The copyright holder is the author/funder. All rights reserved. No reuse without permission. — https://doi.org/10.22541/essoar.167839712.21210255/v1 — This a preprint and has not been peer reviewed. Data may be preliminary.

Hales, T.C., and Roering, J.J., 2007, Climatic controls on frost cracking and implications for the evolution of bedrock landscapes: Journal of Geophysical Research: Earth Surface, v. 112, p. 1–14, doi:10.1029/2006JF000616.

Hales, T.C., Scharer, K.M., and Wooten, R.M., 2012, Southern Appalachian hillslope erosion rates measured by soil and detrital radiocarbon in hollows: Geomorphology, v. 138, p. 121–129, doi:10.1016/j.geomorph.2011.08.030.

Harms, T.K., Rocher-Ros, G., and Godsey, S.E., 2020, Emission of Greenhouse Gases From Water Tracks Draining Arctic Hillslopes: Journal of Geophysical Research: Biogeosciences, v. 125, p. e2020JG005889, doi:10.1029/2020JG005889.

Harris, C., Davies, M.C.R., and Coutard, J.-P., 1997, Rates and processes of periglacial solifluction: an experimental approach: Earth Surface Processes and Landforms, v. 22, p. 849–868, doi:10.1002/(SICI)1096-9837(199709)22:9<849::AID-ESP784>3.0.CO;2-U.

Hinzman, L.D., Kane, D.L., Gieck, R.E., and Everett, K.R., 1991, Hydrologic and thermal properties of the active layer in the Alaskan Arctic: Cold Regions Science and Technology, v. 19, p. 95–110, doi:10.1016/0165-232X(91)90001-W.

Hirst, C., Mauclet, E., Monhonval, A., Tihon, E., Ledman, J., Schuur, E.A.G., and Opfergelt, S., 2022, Seasonal Changes in Hydrology and Permafrost Degradation Control Mineral Element-Bound DOC Transport From Permafrost Soils to Streams: Global Biogeochemical Cycles, v. 36, doi:10.1029/2021GB007105.

Hurst, M.D., Mudd, S.M., Yoo, K., Attal, M., and Walcott, R., 2013, Influence of lithology on hillslope morphology and response to tectonic forcing in the northern Sierra Nevada of California: Journal of Geophysical Research: Earth Surface, v. 118, p. 832–851, doi:10.1002/jgrf.20049.

Istanbulluoglu, E., and Bras, R.L., 2005, Vegetation-modulated landscape evolution: Effects of vegetation on landscape processes, drainage density, and topography: Journal of Geophysical Research: Earth Surface, v. 110, p. 1–19, doi:10.1029/2004JF000249.

Jorgenson, M.T., Romanovsky, V., Harden, J., Shur, Y., O'Donnell, J., Schuur, E.A.G., Kanevskiy, M., and Marchenko, S., 2010, Resilience and vulnerability of permafrost to climate change: Canadian Journal of Forest Research, v. 40, p. 1219–1236, doi:10.1139/X10-060.

Kane, D.L., Hinkel, K.M., Goering, D.J., Hinzman, L.D., and Outcalt, S.I., 2001, Non-conductive heat transfer associated with frozen soils: Global and Planetary Change, v. 29, p. 275–292, doi:10.1016/S0921-8181(01)00095-9.

Kane, D.L., Hinzman, L.D., Benson, C.S., and Everett, K.R., 1989, Hydrology of Imnavait Creek, an Arctic Watershed: Holarctic Ecology, v. 12, p. 262–269.

Kirkby, M.J., 1995, A Model for Variations in Gelifluction Rates with Temperature and Topography : Implications for Global Change: Geografiska Annaler, Series A: Physical Geography, v. 77, p. 269–278.

Lamontagne-Halle, P., McKenzie, J.M., Kurylyk, B.L., and Zipper, S.C., 2018, Changing groundwater discharge dynamics in permafrost regions: Environmental Research Letters, v. 13, p. 084017, doi:10.1088/1748-9326/aad404.

Levy, J.S., Fountain, A.G., Gooseff, M.N., Welch, K.A., and Lyons, W.B., 2011, Water tracks and permafrost in Taylor Valley, Antarctica: Extensive and shallow groundwater connectivity in a cold desert ecosystem: Bulletin of the Geological Society of America, v. 123, p. 2295–2311, doi:10.1130/B30436.1.

Levy, J.S., and Johnson, J.T.E., 2021, Remote soil moisture measurement from drone-borne reflectance spectroscopy: Applications to hydroperiod measurement in desert playas: Remote Sensing, v. 13, doi:10.3390/rs13051035.

Posted on 9 Mar 2023 — The copyright holder is the author/funder. All rights reserved. No reuse without permission. — https://doi.org/10.22541/essoar.167839712.21210255/v1 — This a preprint and has not been peer reviewed. Data may be preliminary.

Lewkowicz, A.G., 2007, Dynamics of Active-layer Detachment Failures, Fosheim Peninsula, Ellesmere Island, Nunavut, Canada Antoni: Permafrost and Periglacial Processes, v. 18, p. 89–103, doi:10.1002/ppp.578.

Lewkowicz, A.G., and Harris, C., 2005, Frequency and Magnitude of Active-layer Detachment Failures in Discontinuous and Continuous Permafrost , Northern Canada: Geomorphology, v. 130, p. 115–130, doi:10.1002/ppp.522.

Lewkowicz, A.G., and Way, R.G., 2019, Extremes of summer climate trigger thousands of thermokarst landslides in a High Arctic environment: Nature Communications, v. 10, p. 1–11, doi:10.1038/s41467-019-09314-7.

Littlefair, C.A., Tank, S.E., and Kokelj, S.V., 2017, Retrogressive thaw slumps temper dissolved organic carbon delivery to streams of the Peel Plateau, NWT, Canada: Biogeosciences, v. 14, p. 5487–5505, doi:10.5194/bg-14-5487-2017.

Litwin, D.G., Tucker, G.E., Barnhart, K.R., and Harman, C.J., 2022, Groundwater Affects the Geomorphic and Hydrologic Properties of Coevolved Landscapes: Journal of Geophysical Research: Earth Surface, v. 127, p. e2021JF006239, doi:10.1029/2021JF006239.

Luoto, M., 2007, New Insights into Factors Controlling Drainage Density in Subarctic Landscapes: Arctic, Anarctic and Alpine Research, v. 39, p. 117–126.

Matsuoka, N., 2001, Solifluction rates, processes and landforms: A global review: Earth-Science Reviews, v. 55, p. 107–134, doi:10.1016/S0012-8252(01)00057-5.

Mcnamara, J.P., Kane, D.L., and Hinzman, L.D., 1999, An analysis of an arctic channel network using a digital elevation model: Geomorphology, v. 29, p. 339–353.

Mudd, S.M., Clubb, F.J., Grieve, S.W.D., Milodowski, D.T., Gailleton, B., Hurst, M.D., Valters, D.A., Wickert, A.D., and Hutton, E.W.H., 2021, LSDTopoTools2:, https://doi.org/10.5281/zenodo.5788576.

Myers-Smith, I.H. et al., 2011, Shrub expansion in tundra ecosystems: Dynamics, impacts and research priorities: Environmental Research Letters, v. 6, doi:10.1088/1748-9326/6/4/045509.

Paquette, M., Fortier, D., and Vincent, W.F., 2017, Water tracks in the High Arctic: a hydrological network dominated by rapid subsurface flow through patterned ground: Arctic Science, v. 3, p. 334–353, doi:10.1139/as-2016-0014.

Parker, R.N., Hales, T.C., Mudd, S.M., Grieve, S.W.D., and Constantine, J.A., 2016, Colluvium supply in humid regions limits the frequency of storm-triggered landslides: Scientific Reports, v. 6, p. 1–7, doi:10.1038/srep34438.

Perron, J.T., 2017, Climate and the Pace of Erosional Landscape Evolution: Annual Review of Earth and Planetary Sciences, v. 45, p. 561–591.

Porter, C. et al., 2018, ArcticDEM: Harvard Dataverse, V1, https://doi.org/10.7910/DVN/OHHUKH,.

Reneau, S.L., and Dietrich, W.E., 1991, Erosion rates in the southern oregon coast range: Evidence for an equilibrium between hillslope erosion and sediment yield: Earth Surface Processes and Landforms, v. 16, p. 307–322, doi:10.1002/esp.3290160405.

Rowland, J.C. et al., 2010, Arctic landscapes in transition: Responses to thawing permafrost: Eos, doi:10.1029/2010EO260001.

Sangireddy, H., Carothers, R.A., Stark, C.P., and Passalacqua, P., 2016, Controls of climate, topography, vegetation, and lithology on drainage density extracted from high resolution topography data: Journal of Hydrology, v. 537, p. 271–282, doi:10.1016/j.jhydrol.2016.02.051.

Posted on 9 Mar 2023 — The copyright holder is the author/funder. All rights reserved. No reuse without permission. — https://doi.org/10.22541/essoar.167839712.21210255/v1 — This a preprint and has not been peer reviewed. Data may be preliminary.

Schwab, M.S., Hilton, R.G., Raymond, P.A., Haghipour, N., Amos, E., Tank, S.E., Holmes, R.M., Tipper, E.T., and Eglinton, T.I., 2020, An Abrupt Aging of Dissolved Organic Carbon in Large Arctic Rivers: Geophysical Research Letters, v. 47, p. e2020GL088823, doi:10.1029/2020GL088823.

Shakil, S., Tank, S.E., Vonk, J.E., and Zolkos, S., 2022, Low biodegradability of particulate organic carbon mobilized from thaw slumps on the Peel Plateau, NT, and possible chemosynthesis and sorption effects: Biogeosciences, v. 19, p. 1871–1890, doi:10.5194/bg-19-1871-2022.

Shelef, E. et al., 2017, Large uncertainty in permafrost carbon stocks due to hillslope soil deposits: Geophysical Research Letters, v. 44, p. 6134–6144, doi:10.1002/2017GL073823.

Suzuki, S., Kankaku, Y., Imai, H., and Osawa, Y., 2012, Overview of ALOS-2 and ALOS-3: Proc. SPIE 8528, Earth Observing Missions and Sensors: Development, Implementation, and Characterization II, doi:doi:10.1117/12.979184.

Tananaev, N., 2022, Defrosting northern catchments: Fluvial effects of permafrost degradation: , p. 20.

Trochim, E.D., Jorgenson, M.T., Prakash, A., and Kane, D.L., 2016, Geomorphic and biophysical factors affecting water tracks in northern Alaska: Earth and Space Science, p. 123–141, doi:10.1002/2015EA000111.

Tucker, G.E., and Bras, R.L., 1998, Hillslope processes, drainage density, and landscape morphology: Water Resources, v. 34, p. 2751–2764.

Turetsky, M. et al., 2020, Carbon release through abrupt permafrost thaw: Nature Geoscience, doi:10.1038/s41561-019-0526-0.

Walker, M., Walker, D.A., and Everett, K.R., 1989, Wetland soils and vegetation, arctic foothills, Alaska: US Department of the Interior, Fish and Wildlife Service, Research and Development.

Walvoord, M.A., and Kurylyk, B.L., 2016, Hydrologic impacts of thawing permafrost—a review: Vadose Zone Journal, v. 15, doi:10.2136/vzj2016.01.0010.

Witharana, C., Udawalpola, M.R., Liljedahl, A.K., Jones, M.K.W., Jones, B.M., Hasan, A., Joshi, D., and Manos, E., 2022, Automated Detection of Retrogressive Thaw Slumps in the High Arctic Using High-Resolution Satellite Imagery: Remote Sensing, v. 14, p. 4132, doi:10.3390/rs14174132.

Wohl, E., 2018, The challenges of channel heads: Earth-Science Reviews, v. 185, p. 649–664, doi:10.1016/j.earscirev.2018.07.008.

Yoo, K., Amundson, R., Heimsath, A.M., and Dietrich, W.E., 2005, Erosion of upland hillslope soil organic carbon: Coupling field measurements with a sediment transport model: Global Biogeochemical Cycles, v. 19, p. 1–17, doi:10.1029/2004GB002271.